

# Challenge of Forecasting Urban Weather with NWP Models

Fei Chen<sup>1</sup>, Yubao Liu<sup>1</sup>, Hiroyuki Kusaka<sup>1,4</sup>, Mukul Tewari<sup>1</sup>, Jian-Wen Bao<sup>2</sup>  
Chun Fung Lo<sup>3</sup>, and Kai Hon Lau<sup>3</sup>

<sup>1</sup> National Center for Atmospheric Research, Boulder, CO

<sup>2</sup> National Oceanic and Atmospheric Administration (NOAA), Boulder, CO

<sup>3</sup> Hong Kong University of Science and Technology, Hong Kong

<sup>4</sup> Central Research Institute of Electric Power Industry (CRIEPI), Abiko, Japan

## 1. INTRODUCTION

Mesoscale numerical weather prediction (NWP) models in connection with increasing capacities of computers in the last few years have considerably increased the spatial (vertical and horizontal) resolution. It is uncommon that some NWP models run with a grid-spacing of 0.5-1 km for local and regional weather forecasts. At such fine scales, the role of urban landuse in local and regional weather needs to be represented in these models and it is important for NWP models to capture effects of urban on wind, temperature, and humidity in the boundary layer and their influences on the boundary layer depth. Not only these boundary layer weather variables influence people's daily life in the urban region, but also they are important input for air dispersion and quality models, which will benefit from improved prediction of the urban meteorological conditions. Having a consistent treatment of the planetary boundary layer structure and evolution in meteorological and air quality models is imperative. Errors in the improper parameterization of urban landuse result in bias in forecasted boundary layer variables and further in predicting the temperature and wind fields.

The spatial distribution of urban landuse (e.g., building height, geometry) is highly heterogeneous even across urban scales.

To explicitly solve the motions around an individual building or buildings requires the use of computational fluid dynamics (CFD) models, which are computationally intensive. Hence, in the foreseeable future, NWP models have to parameterize the subgrid-scale urban variability. Even in this context, it is not clear that which degree of complexity of urban landuse treatment should be incorporated in NWP models. For instance, Taha (1999) preferred a simple approach and pointed out that a large amount of detail in complex urban models may be lost when averaging back to a coarse model grid.

In this paper, we report recent progress in urban landuse modeling for the community MM5 and WRF models. The goals of these efforts are to 1) capture important aspects of momentum, heat, and moisture transfer mechanisms caused by urban landuse, 2) assess the proper degree of complexity in urban treatment for NWP models applied with a grid spacing of 1-5 km, and 3) improve forecasted boundary layer structures over urban regions.

Two different approaches were tested: 1) simply modifying the values of albedo, roughness length, soil thermal properties, and evaporation for the urban landuse in the Unified Noah land surface model (LSM), and 2) coupling a single-layer urban canopy model with the Noah LSM, which considers the 2-D geometry of building and roads to represent the radiation trapping and wind shear in the urban canopy.

---

\* Corresponding author address: Fei Chen, NCAR, PO Box 3000, Boulder, CO 80307; email: feichen@ucar.edu

Liu et al. (2004) applied the first approach in the realtime MM5 operational support system for the 2003 Joint Urban Atmospheric Dispersion Study field experiment. This approach was also applied to investigate the interactions between urban heat island and sea-breeze circulations in the Hong Kong area. Kusaka et al. (2004) employed the second approach in the Weather Research and Forecast (WRF) model in a numerical experiment for the Houston metropolitan region with detailed urban landuse classification.

## 2. MODELING URBAN LANDUSE AND HEAT ISLAND EFFECTS

### 2.1 SIMPLE TREATMENT OF THE URBAN LANDUSE IN MM5/NOAH

The Noah LSM used in MM5 (Chen and Dudhia, 2001) has an overly simplified urban representation, which merely increases the roughness length and reduces surface albedo for urban landuse. Recently, a bulk parameterization for urban landuse has been incorporated in the Noah LSM (Liu et al., 2004). It includes: 1) increasing the roughness length from 0.5 m to 0.8 m to represent turbulence generated by roughness elements and drag due to buildings; 2) reducing surface albedo from 0.18 to 0.15 to represent the shortwave radiation trapping in the urban canyons; 3) using a larger volumetric heat capacity of  $3.0 \text{ J m}^{-3} \text{ K}^{-1}$  for the urban surface (walls, roofs, and roads) which is usually consisted of concrete or asphalt materials; 4) increasing the value of soil thermal conductivity to  $3.24 \text{ W m}^{-1} \text{ K}^{-1}$  to parameterize large heat storage in the urban surface and underlying surfaces, and 5) reducing green vegetation fraction over urban city to decrease evaporation.

### 2.2 SINGLE-LAYER URBAN CANOPY MODEL IN WRF/NOAH

The Noah LSM (Ek et al. 2004) has been recently coupled to the Weather Research and Forecasting (WRF) model (Tewari et al. 2004). We developed a coupled Noah /Urban-

canopy model, based on the single-layer urban canopy model (UCM) of Kusaka et al. (2001). The basic function of an UCM is to take the urban geometry into account in its surface energy budgets and wind shear calculations. Our urban model is based on the urban canopy model developed by Kusaka et al. (2001) and modified by Kusaka and Kimura (2004), which includes: 1) 2-D street canyons that are parameterized to represent the effects of urban geometry on urban canyon heat distribution (Figure 1); 2) shadowing from buildings and reflection of radiation in the canopy layer (Figure 2); 3) the canyon orientation and diurnal cycle of solar azimuth angle, 4) man-made surface consists of eight canyons with different orientation; 5) Inoue's model for canopy flows (Inoue 1963); 6) the multi-layer heat equation for the roof, wall, and road interior temperatures; 7) anthropogenic heating associated with energy consumption by human activities; and 8) a very thin bucket model for evaporation and runoff from road surface.

**Figure 1 Schematic of the Urban Canopy Model.**  $Z_a$ : height of the lowest model level;  $T_a$ : air temperature at  $Z_a$ ;  $H$ : aggregated sensible heat flux;  $Z_r$ : building height;  $Z_T$ : roughness length for heat;  $d$ : zero displacement height.  $T_R$ ,  $T_W$ , and  $T_G$  are surface temperature of roof, wall, and road, respectively; and  $H_R$ ,  $H_a$ ,  $H_W$ , and  $H_G$  are sensible heat fluxes from the roof, canyon, wall, and road, respectively.

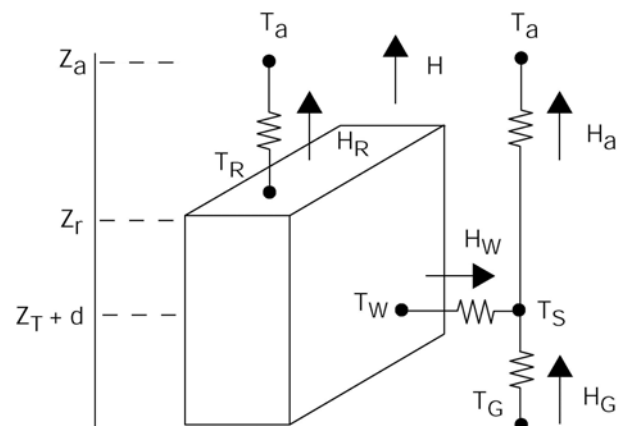
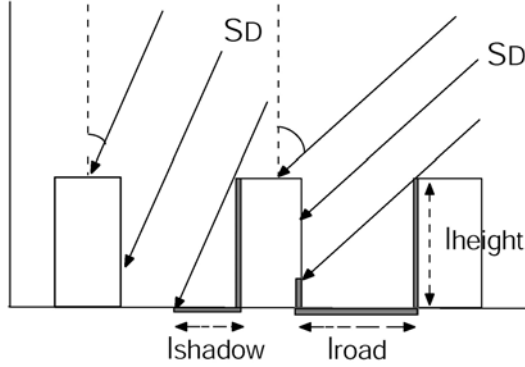


**Figure 2: Shortwave downward radiation in the urban street canyon.**  $l_{\text{shadow}}$  and  $l_{\text{road}}$  are the lengths of shading on the road.  $l_{\text{height}}$  is the building height.

( i )  $l_{\text{shadow}} < l_{\text{road}}$     ( ii )  $l_{\text{shadow}} > l_{\text{road}}$



This urban canopy model takes into account sensible heat fluxes from roof, wall, and road; and then aggregated them into energy and momentum exchange between the urban surface and the atmosphere. Various heat fluxes illustrated on Figure 1 are estimated by the Monin-Obkhov similarity theory or by the Jurges formula used in the architectural field. Surface temperature is calculated from the upward long wave radiation, which is the difference between the net long wave radiation and downward long wave radiation. The net long wave radiations are calculated from the following equation:

$$L_R = \varepsilon_R \left( L^\downarrow - \sigma T_R^4 \right),$$

$$L_{W,1} = \varepsilon_W \left( L^\downarrow F_{W \rightarrow S} + \varepsilon_G \sigma T_G^4 F_{W \rightarrow G} + \varepsilon_W \sigma T_W^4 F_{W \rightarrow W} - \sigma T_W^4 \right),$$

$$L_{W,2} = \varepsilon_W \left[ (1 - \varepsilon_G) L^\downarrow F_{G \rightarrow S} F_{W \rightarrow G} + (1 - \varepsilon_G) \varepsilon_W \sigma T_W^4 F_{G \rightarrow W} F_{W \rightarrow G} \right. \\ \left. + (1 - \varepsilon_W) L^\downarrow F_{W \rightarrow S} F_{W \rightarrow W} + (1 - \varepsilon_W) \varepsilon_G \sigma T_G^4 F_{W \rightarrow G} F_{W \rightarrow W} \right. \\ \left. + \varepsilon_W (1 - \varepsilon_W) \sigma T_W^4 F_{W \rightarrow W} F_{W \rightarrow W} \right],$$

$$L_{G,1} = \varepsilon_G \left[ L^\downarrow F_{G \rightarrow S} + \varepsilon_W \sigma T_W^4 F_{G \rightarrow W} - \sigma T_G^4 \right],$$

$$L_{G,2} = \varepsilon_G \left[ (1 - \varepsilon_W) L^\downarrow F_{W \rightarrow S} F_{G \rightarrow W} \right. \\ \left. + (1 - \varepsilon_W) \varepsilon_G \sigma T_G^4 F_{W \rightarrow G} F_{G \rightarrow W} + \varepsilon_W (1 - \varepsilon_W) \sigma T_W^4 F_{W \rightarrow W} F_{G \rightarrow W} \right].$$

Here  $L^\downarrow$  is the downward atmospheric long wave radiation. The sky view factors,  $F$ , is computed in the same way as Kusaka et al. (2001). Subscripts  $W$ ,  $G$ , and  $S$  denote wall,

ground (road), and sky, respectively. For instance,  $F_{G \rightarrow S}$  means the sky view factor from the road. Subscripts 1 and 2 refer to the absorption of the direct and reflected radiation, respectively. The set of parameters required by this UCM is described in Table 1.

**Table 1: Parameters for the single-layer urban canopy model**

Parameter	Symbol	Unit
Urban type	<i>Urban</i>	
	<i>type</i>	
Roof level (building height)	$z_R$	[ m ]
Roof area ratio (Building coverage ratio)	$A_R$	
Wall area ratio	$A_W$	
Road area ratio	$A_G$	
Volumetric heat capacity of roof	$\rho C_R$	[ J m <sup>-3</sup> K <sup>-1</sup> ]
Volumetric heat capacity of wall	$\rho C_W$	[ J m <sup>-3</sup> K <sup>-1</sup> ]
Volumetric heat capacity of road	$\rho C_G$	[ J m <sup>-3</sup> K <sup>-1</sup> ]
Thermal conductivity of roof	$\lambda_R$	[ W m <sup>-1</sup> K <sup>-1</sup> ]
Thermal conductivity of wall	$\lambda_W$	[ W m <sup>-1</sup> K <sup>-1</sup> ]
Thermal conductivity of road	$\lambda_G$	[ W m <sup>-1</sup> K <sup>-1</sup> ]
Sub-layer Stanton number	$B_H^{-1}$	
Roughness length	$z_0$	[ m ]
Roughness length above canyon	$z_{0C}$	[ m ]
Roughness length above roof	$z_{0R}$	[ m ]
Zero plane displacement height	$d$	[ m ]
Roof surface albedo	$\alpha_R$	
Wall surface albedo	$\alpha_W$	
Road surface albedo	$\alpha_G$	
Roof surface emissivity	$\varepsilon_R$	

Wall surface emissivity	$\epsilon_W$
Road surface emissivity	$\epsilon_G$
Moisture availability of roof	$\beta_R$
Moisture availability of road	$\beta_G$

It is necessary to estimate heat transfer from the natural surface (parks, recreation areas, etc.) when a grid cell is not fully covered by urban 'artificial' surface. Hence, this UCM is coupled to Noah through a parameter 'urban percentage',  $U_p$ , to represent urban sub-grid scale heterogeneity, which can be estimated by fine-scale satellite images. Hence, the aggregated grid-grid-scale sensible heat flux, for example, can be estimated as follows:

$$H = (1 - U_p) \times H_{LSM} + U_p \times H_{UCM}$$

Here,  $H$  is the total sensible heat flux from an 'urban' grid cell to the atmospheric surface layer,  $U_p$  is the area ratio of a man-made urban surface, and  $(1 - U_p)$  represents natural surface such as grassland, farmland, and

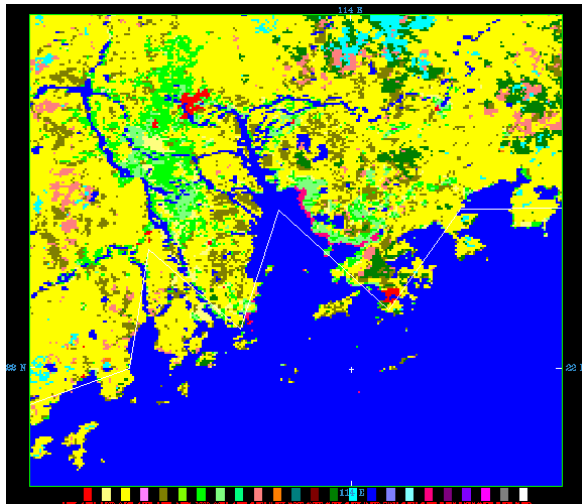
trees.  $H_{LSM}$  is the sensible heat flux from the Noah LSM for natural surfaces, while  $H_{URBAN}$  is the sensible heat flux from UCM for artificial surfaces. Latent heat flux and upward long wave radiation flux from a grid cell are treated in a similar way.

### 2.3 REPRESENTING URBAN LANDUSE DISTRIBUTION IN NWP MODELS

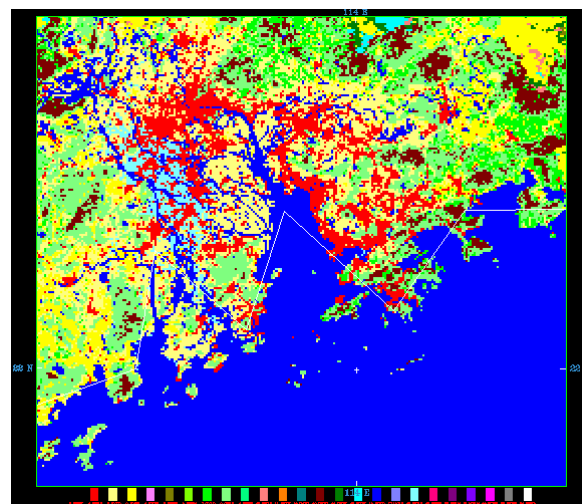
Regardless of the complexity of urban landuse models, the first challenge in NWP urban landuse modeling is to accurately characterize the extent of urban areas. This has to rely on the use of remote sensing data for specifying large urban areas. However, due to the differences in algorithms used to identify urban and rapid growth of urban areas in certain regions, different data sources may reveal different urban coverage. Sometimes, it is therefore necessary to adjust the urban areas using field survey data.

As shown on **Figure 3**, the urban area for the Pearl River Delta region adjusted by local urban planning maps is much larger and more realistic than the one based 1994 USGS landuse map.

**Figure 3: Urban areas over the Pearl River Delta region (China)**

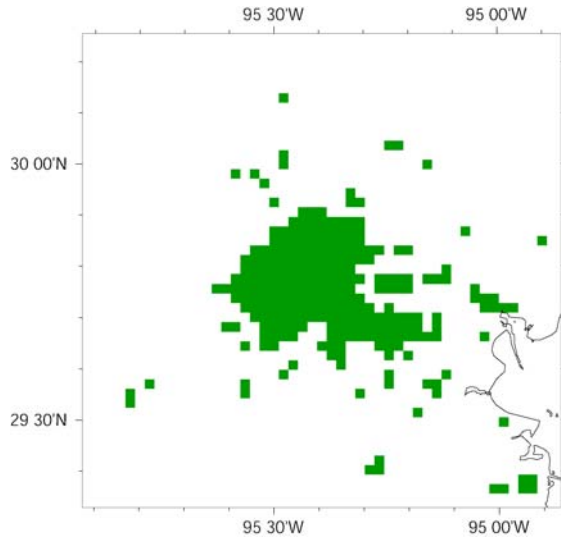


a: Urban (in red) area defined by the 1-km USGS 24-category landuse map.

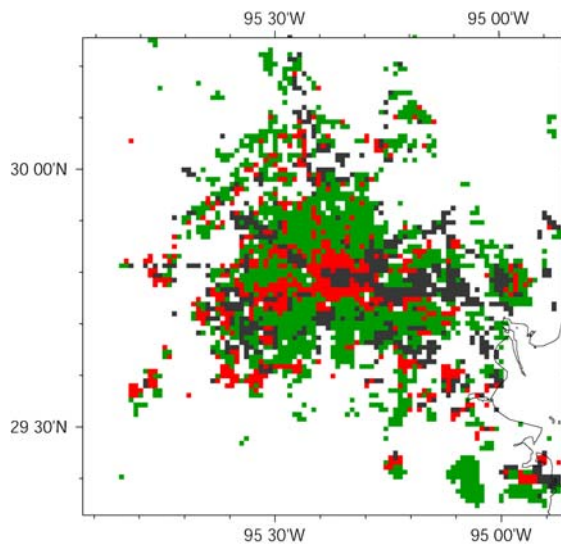


b: Urban area (in red) based on local landuse map obtained from Hong Kong City Planning Office.

**Figure 4. Urban areas over the Houston metropolitan region.**



a) Houston urban extent defined by the 1-km USGS landuse map. green: urban



b) Houston urban extent based on the USGS/EPA 30-m Landsat based landuse map. green: low-intensity residential area, red: high-intensity residential area, and black: commercial/industrial.

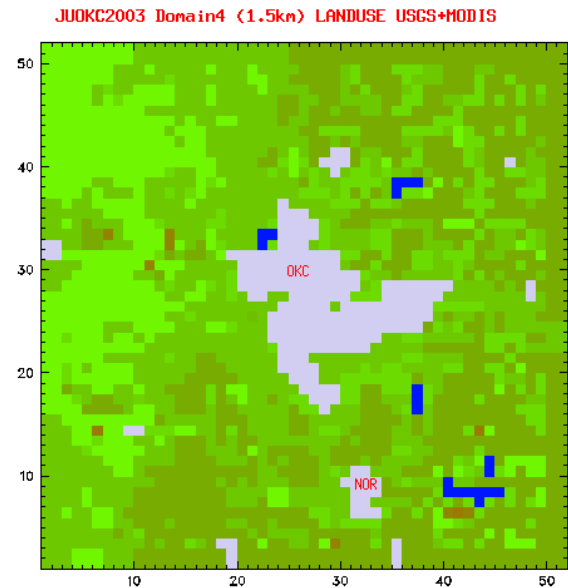
Another example is shown on Figure 4 for the Houston metropolitan region, which again shows larger urban area by using the 30-m Landsat based map adjustment. While the simple one-category urban classification (as in **Figure 3** and Figure 4a) are useful for the bulk parameterization of urban landuse modeling, the more detailed urban classification (Figure 4b) is critical for defining

urban geometry, hydrologic characteristics, and subgrid-scale natural landuse fraction required by more sophisticated urban canopy model.

## 2.4 RESULTS FROM A SIMPLE URBAN LANDUSE MODELING APPROACH WITH THE NOAH LAND SURFACE MODEL

Liu et al. (2004) described the use of the simple urban landuse model in the Noah LSM in the MM5 based Real-Time Four-Dimensional data Assimilation (RTFDDA) and forecast system. This RTFDDA system was used to support the Joint Urban 2003 Atmospheric Dispersion Study (JU2003), held in Oklahoma City (OKC), Oklahoma, in July 2003. In the high-resolution 5-domain RTFDDA configuration, the urban area occupies roughly 20% of the 1.5-km grid (domain 4 see Figure 5) and 70% of the 0.5-km grid (domain 5).

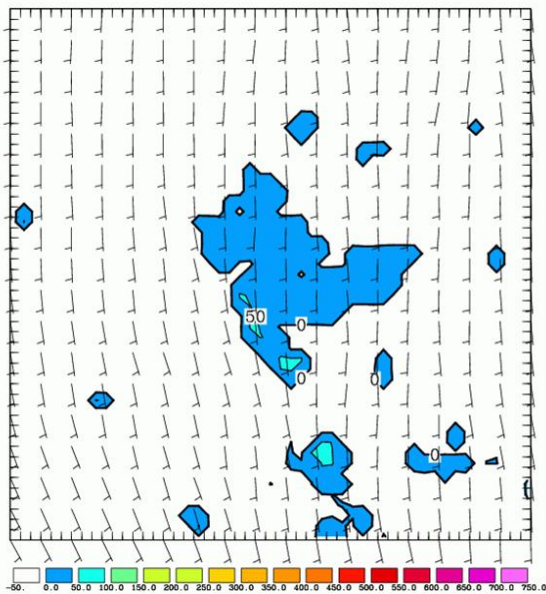
**Figure 5 Oklahoma city and Norman urban areas shown on MM5 1.5-km grid, based on 1-km USGS landuse map and aerial photo.**



In MM5 simulations of Liu et al. (2004), the 'urban heat island' effects seem prominent in the 9-day average of 1.5-km grid RTFDDA forecasts, as the OKC area is roughly two or three degrees warmer than the rural regions.

In fact, the nocturnal surface temperature was warmer than the air temperature over urban and resulted in positive surface sensible heating (Figure 6), while the surrounding rural areas are mostly in the stable regime because of surface inversion. That changes the nocturnal boundary layer regime from unstable to slightly convective. Qualitatively, the simulated positive surface sensible heat fluxes and deeper PBL are confirmed by OKC field observations conducted in the city canyon (Gouveia et al., 2004).

**Figure 6** Sensible heat fluxes averaged for nine-clear sky-day days July 2003 RTFDDA forecasts valid at 06 UTC (about local midnight).

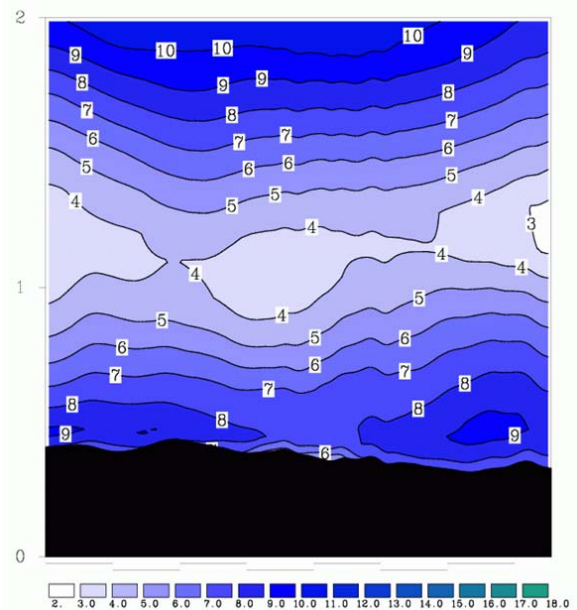
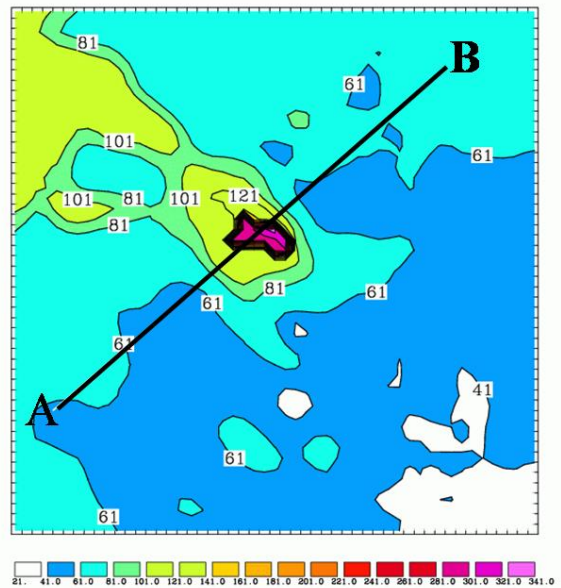


Examination of daily RTFDDA forecasts revealed more pronounced influences of urban landuse on the atmosphere (Figure 7). For instance, the PBL height over the core OKC urban region was about 100 meters higher than that over the rural regions. Due to stronger mixing in the 'nocturnal convective mixed layer' and hence less decoupling of surface layer with the atmosphere, the strength of low level jet over the OKC is weaker than that in the surrounding areas.

Daytime PBL height over OKC area was about 200 to 300 meters higher than that over rural areas, and organized mesoscale circulations seem to develop as a result of

differential heating and pressure gradients between urban and rural areas, forming convergence over the urban region. This influx of moisture from more moist rural area over the strongly mixed boundary layer over the urban makes the urban entrainment zone saturated more easily (not shown here).

**Figure 7** PBL height (upper plot in meters) and wind speed (in  $\text{ms}^{-1}$ ) at the lowest 2 km (lower plot) along the AB cross section, valid at 06 UTC June 24, 2003.



## 2.5 RESULTS FROM NOAH/UCM COUPLED MODEL WITH WRF

The single-layer UCM of Kusaka et al. (2001, 2004) has been coupled to the Noah LSM in WRF, and this coupled system is being tested for the Houston urban areas. To take a full advantage of this relatively complex UCM, a more detailed urban classification map is used in our WRF simulations, which divides the urban areas into three categories: 1) low intensity residential area, 2) high-intensity residential area, and 3) commercial/industrial area (See Figure 4b).

We selected the 25 August 2000 as our first case to apply this coupled WRF system. The case was chosen because it was cloudy ahead of the sea-breeze front followed by clearing in the late afternoon after the front passes. Hence, it represents a potentially interesting case in which the strength of urban heat island can modify the evolution of sea-breeze and impact the air quality in the Houston region. Also there are data collected during the Texas Air Quality Study 2000 (TEXAQS 2000) that we can use to evaluate the model. In the preliminary test presented in this paper, WRF model, with 4-km grid spacing, was run for a 24-hour simulation initialized at 12Z 25 August 2000.

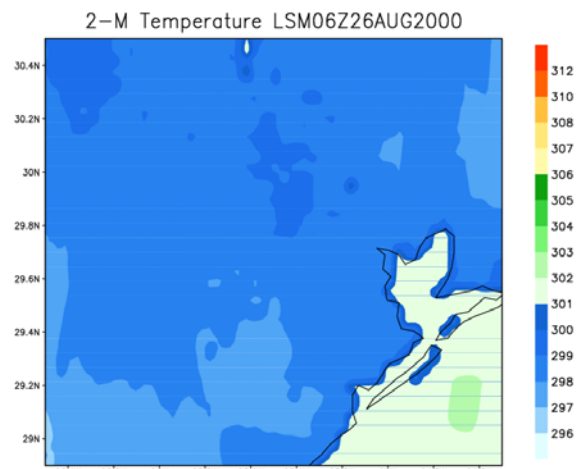
The nighttime 2-meter air temperature simulated with UCM is 10 degrees higher than that simulated with the Noah LSM without urban treatment, and than the surrounding rural areas (Figure 8). More interestingly, the simulation with UCM, together with a detailed urban classification map, was able to produce the often observed temperature distribution within an urban heat island. That is: higher temperature is found in high-intensity residential area, because of larger building coverage, is usually higher than that in low-intensity residential areas.

Further investigations reveal that the fine-scale temperature distributions are larger determine by the wall temperature distribution (Figure 9b). Presumably, this is because building walls absorb more downward solar

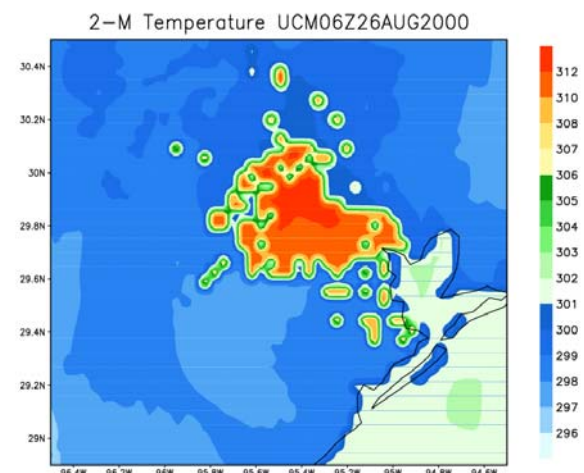
radiation due to radiation trapping than roads, and have deeper heat storage layer and large thermal capacity than roofs.

More simulations with higher resolution (2-km grid spacing) are underway to study the sensitivity of various UCM parameters and their influences on urban boundary layer structures. Observations from TEXAQS 2000 will be used to evaluate these simulations.

**Figure 8. WRF simulated air temperature at 2 meter valid at 06Z 26 August 2000.**

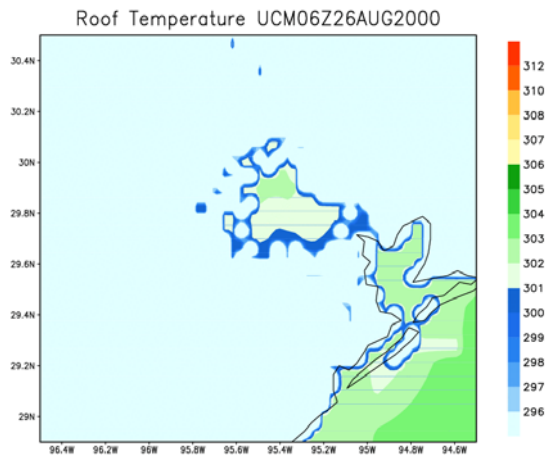


a) Simulation with the Noah LSM without urban treatment.

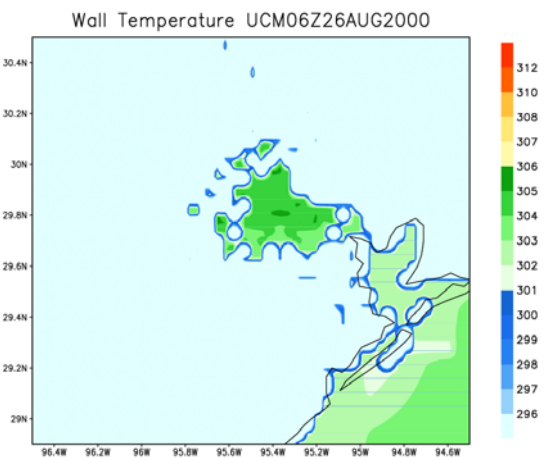


b) Simulation with the Noah LSM coupled with UCM

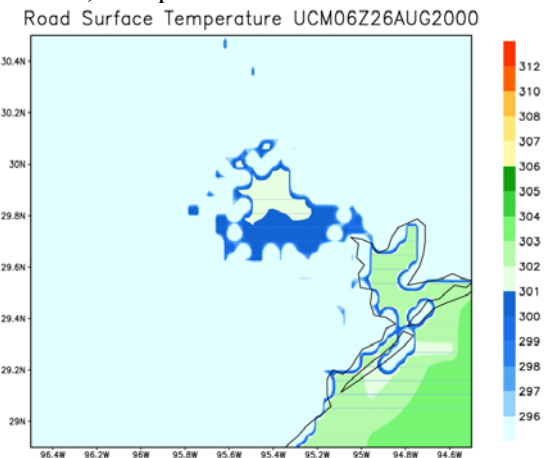
**Figure 9. Surface temperature from the urban canopy model valid at 06Z 26 August 2000. Also shown is the sea surface temperature.**



a) Temperature at the roof top.



b) Temperature at the wall surface.



c) Temperature at the road surface.

### 3. SUMMARY

Nowadays NWP models with 0.5-1 km grid spacing have been used for local forecasts, and this type of fine grid spacing is likely to be used for NWP at continental-scale in the near future. Capturing fine-scale influences of urban heat island becomes increasingly important. Described in this paper are recent modeling results that utilized a simple ‘bulk’ urban landuse treatment in MM5, and a more complex urban canopy model in WRF with a more detailed description of urban landuse types.

The MM5 model simulations for the OKC reproduced some observed nocturnal urban heat island features, namely: higher urban temperature, deeper boundary layer, slightly convective surface layer, reduction of wind speed. However, the simulated surface and boundary layer structures are homogeneous, albeit a distortion of such homogeneity by advection, over the entire urban areas because of inherent constrains in its overly simplified urban model. On the other hand, WRF simulations conducted with an UCM and multiple urban landuse types produced some interesting fine-scale atmospheric structures reflecting the underlying thermal characteristics of urban buildings, walls, and roads.

As far as urban canopy models are concerned, the degree to which we can improve the prediction of urban boundary layer structures depends on how well we: 1) understand the statistical characteristics of turbulent transfer of heat/momentum from urban canyon to the atmosphere because of possible gaps in representing scales of motions, 2) characterize the urban landuse at fine-scales, 3) define important parameters in complex UCMs, and 4) initialize the temperature profiles in buildings, walls, and roads. Much of the future improvements will rely on the utilization of new remotely-sensed data and field observation data.

Should these features simulated by the WRF/Noah/UCM are confirmed by observations, this type of coupled models, along with multiple urban types, will be useful to improve longterm (beyond a few hours) urban weather forecasts, which are practically absent in current NWP models. More accurate predication of boundary layer structures in a city and in rural areas will certainly improve our ability to predict air quality and dispersion for important homeland security applications.

#### 4. REFERENCES

Chen, F., and J. Dudhia, 2001: Coupling an advanced land-surface/hydrology model with the Penn State/NCAR MM5 modeling system. Part I: Model implementation and sensitivity. *Mon. Wea. Rev.*, **129**, 569-585.

Ek, MB., K.E. Mitchell, Y. Lin, E. Rogers, P. Grummann, V. Koren, G. Gayno, and J. D. Tarpley, 2003: Implementation of Noah land-surface model advances in the NCEP operational mesoscale Eta mode . *J. Geophys. Res.*, **108** (D22): No. 8851 NOV 29.

Gouveia, F.J, M.J. Leach, J.H. Shinn, 2004: Measurements of net radiation, ground heat flux and surface temperature in an urban canyon. Symposium on "Planning, Nowcasting, and Forecasting in the Urban Zone". 1-15 January, Seattle, WA.

Kusaka, H., H. Kondo, Y. Kikegawa, and F. Kimura, 2001: A simple single-layer urban canopy model for atmospheric models: Comparison with multi-layer and slab models. *Bound.-Layer Meteorol.*, **101**, 329-358.

Kusaka, H. and F. Kimura, 2004: Coupling a single-layer urban canopy model with a simple atmospheric model: Impact on urban heat island simulation for an idealized case. *Journal of the Meteorological Society of Japan*, **82**, 67-80.

Kusaka, H., F. Chen, J.W. Bao, and H. Hirakuchi, 2004: Simulation of the urban heat island effects over the Greater Houston Area

with the high resolution WRF/LSM/Urban coupled system. Symposium on "Planning, Nowcasting, and Forecasting in the Urban Zone". 1-15 January, Seattle, WA.

Liu, Y., F. Chen, T. Warner, S. Swerdlin, J. Bowers, and S. Halvorson, 2004: Improvements to surface flux computations in a non-local-mixing PBL scheme, and refinements on urban processes in the Noah land-surface model with the NCAR/ATEC real-time FDDA and forecast system. 20th Conference on Weather Analysis and Forecasting/16th Conference on Numerical Weather Prediction. 11-15 January, 2004, Seattle, Washington.

Taha, H.: 1999, 'Modifying a Mesoscale Meteorological Model to Better Incorporate Urban Heat Storage: A Bulk-Parameterization Approach', *J. Appl. Meteorol.* **38**, 466-273.

Tewari., M., F. Chen, W. Wang, J. Dudhia, M. LeMone, K. Mitchell, M. Ek, G. Gayno, J. Wegiel, and R. Cuenca, 2004: Implementation and verification of the unified Noah land surface model in the WRF model. 20th Conference on Weather Analysis and Forecasting/16th Conference on Numerical Weather Prediction. 11-15 January, 2004, Seattle, Washington.